

EML webinar overview: Elastic Strain Engineering for unprecedented properties



Ju Li

Department of Nuclear Science and Engineering, MIT, Cambridge, MA 02139, USA
 Department of Materials Science and Engineering, MIT, Cambridge, MA 02139, USA

ARTICLE INFO

Article history:

Received 6 July 2021

Accepted 8 July 2021

Available online 14 July 2021

Keywords:

Smaller is stronger

Deep elastic strain

First-principles machine-learned (FPML)

constitutive relation

TCAD

MEMS

Kilogram-scale ESE for energy technologies

ABSTRACT

Elastic Strain Engineering (ESE) utilizes all six components of the strain tensor to guide the interactions of material structures with electrons, phonons, etc. and control energy, mass and information flows. The success of Strained Silicon technology today harbingers what deep ESE (>5% elastic strain in a large enough space-time volume) may accomplish for civilization, with likely breakthroughs in electronics, photonics, superconductivity, quantum information processing, etc. In this webinar I give examples of exploiting the strain and strain-gradient design space of nanostructured materials. Inhomogeneous elastic strain patterns lead to dynamically tunable artificial atoms and pseudo-heterostructures to regulate quasiparticle energetics and motion. Strain also governs crystal defect charging levels, carrier effective mass, direct-to-indirect bandgap and band topology transitions, etc. which can be efficiently sampled by quantum mechanical calculations and represented by machine-learning models such as neural network (NN) representations. Technology computer-aided design (TCAD) finite-element simulations with first-principles machine-learned (FPML) constitutive relations coupled to topology optimization (TO) tools are being developed to guide the design of freely suspended, micro-electromechanical system (MEMS) devices in fin-field-effect transistor (FinFET) like geometries. Productions of kilogram-scale nanowire composites and metallic glasses under large tensile elastic strain have also been demonstrated for energy technology applications, that can lead to better superconductors, catalysts and magnets. By controlling the strain patterns, one opens up a much larger parameter space – on par with chemical alloying – for optimizing the functional properties of materials, thus fulfilling Feynman's vision "There's Plenty of Room at the Bottom". EML webinar speakers, videos, and overviews can be found at <https://imechanica.org/node/24098>.

© 2021 Elsevier Ltd. All rights reserved.

Contents

Extended summary with references	1
Pillar 1	2
Pillar 2	2
Pillar 3	2
Pillar 4	3
Declaration of competing interest.....	6
References	6

Extended summary with references

Elastic Strain Engineering (ESE) is mechanical design of material structures to induce large stresses and/or stress gradients, to guide electrons, photons, phonons, etc. and control energy, mass and information flows. High-pressure physics is a subset

of ESE and has revealed some of its potential with just "one-half" (hydrostatic compression direction) of the six stress components. Because "smaller is stronger" [1,2], there is a much larger dynamical range of tensile-and-deviatoric shear stresses that nanomaterials can withstand at room temperature for long time. This trend is often represented by a Hall-Petch type scaling law $\sigma_{\text{shear/tension limit}} = \sigma_0 + kD^{-\alpha}$ where D is the characteristic grain/sample size and α is around 1/2. This effect originates broadly from changes in the defect population dynamics at small

E-mail address: liju@mit.edu.

<https://doi.org/10.1016/j.eml.2021.101430>

2352-4316/© 2021 Elsevier Ltd. All rights reserved.

grain or sample sizes, for example from a defect-propagation controlled strength to a defect-nucleation controlled one [3] at room temperature. For instance, the requisite pinning centers in Frank–Read dislocation sourcing mechanism are not truly immobile, and may be destabilized by interactions with adjacent grain boundaries or surfaces, and once such dislocation sources are thermally or mechanically annealed away [4] to boundaries, glissile dislocations required for plastic deformation would have to be generated afresh at much higher stresses, and so inelastic stress relaxations become much more difficult at small D (with strong qualification on the temperature [5], though).

The term “ultra-strength” was coined in 2009 [6] to describe material components sustaining sample-wide stress level at a significant fraction ($>1/10$ th) of its ideal strength, or $\sim 1\%$ elastic strain [1] pervasively. The qualifier “sample-wide” is important in the ESE context because even in conventional coarse-grained materials, near the extended defect cores the local stress can exceed $1/10$ th of its ideal strength. But a large enough space-time volume (say $\mu\text{m}^3 \times \text{months}$) of good lattice at $>\sigma_{\text{ideal}}/10$, away from defect cores, is needed practically to be truly useful for ESE of functional properties. Therefore the qualification of significant space-time volume of realistic samples that one can obtain experimentally, is important. In recent years, there have been more and more material examples of “deep ESE”: that is, $> \sim 5\%$ elastic strain or $> \sigma_{\text{ideal}}/2$, at room temperature or at a service temperature of interest.

ESE can potentially revolutionize electronics, photonics, superconductivity, catalysis, sensing, etc. applications. Strained silicon is a well-known technology where by depositing Si epitaxially on $\text{Si}_{1-x}\text{Ge}_x$ substrate, the nanoscale Si channel is biaxially stretched up to $\sim 1\%$, to improve the carrier mobilities by as much as 100%. This technology was commercialized in 2000s and is now used extensively in CPUs and GPUs [7]. But deep ESE promises a lot more than mere 100% improvement in performance.

Historically, chemically alloying has played a huge role in our civilization (bronze age \rightarrow iron age \rightarrow silicon age) and is extremely well known. But ESE barely registers in the mass consciousness. This disparity was because successful ESE requires four necessary ingredients, or pillars (Fig. 1), each of which did not become available until a few decades ago:

Pillar 1

Pillar 1 is the ability to fabricate materials structures that can withstand elastic strain patterns that are exceptionally large in amplitude [8], inhomogeneous [9], dynamically reversible [10], or combinations thereof. The crystal ideal strength, first developed by Jacov Frenkel in 1926 [11], is defined as the maximum stress that a perfect crystal – without any defects, not even surfaces – can withstand at zero Kelvin. This notion was later generalized to glasses [12]. Density functional theory (DFT) calculations showed that the ideal strength of crystals is typically $\sim E/10$ in tension or $\sim G/10$ in shear, where E and G are the Young’s modulus or shear modulus in the said crystallographic direction [1]. Before the 1990s, there was only significant experience in the equal triaxial negative stress direction from the high-pressure physics community, that can approach the ideal strength surface. In all the other directions in the 6D strain space, only small regions relative to the ideal strength limits were explored by the mechanics community, in e.g. physical metallurgy and fracture studies, due to the intervention of plastic flow and/or fracture inelastic relaxation mechanisms at relatively low elastic strains (typically less than 0.2%) compared to the 10%–20% level ideal strain limit. However, in the last three decades, there have been an explosion of ultrastrong materials such as thin films, bulk nanocrystals, small-volume materials, metallic glasses, nanowires, nanoparticles and 2D materials, that can

withstand very significant deviatoric and tensile stresses for long time, which greatly opened up the materials repertoire for ESE [6]. They range from metallic alloys, intermetallic compounds, to narrow, mid and wide-bandgap semiconductors, and ceramics, and even soft materials and polymers, with wide range of functional behavior. As an example, in 2007 we predicted based on ab-initio phonon calculations that monolayer graphene will have ideal tensile strength of 120 GPa [13]. A year later, experimental groups at Columbia University verified our prediction quantitatively [14]. From the DFT calculations, we predicted a large phononic bandgap must open up at large tensile strains. Since the thermal conductivity and electron–phonon coupling (which controls thermoelectricity and superconductivity) all depend on phonons, such huge change in the phonon band structure means that “9% stretched graphene” is very different from normal graphene, and “9% sheared” graphene is also very different from “9% stretched” graphene. Given how much research efforts and interesting physical behaviors have been seen in normal graphene, strained graphene may lead to many more discoveries [15].

Pillar 2

Pillar 2 is the ability to induce large elastic strains locally [15–17], and measure on the spot how the material’s physico-chemical properties change, i.e. how conductivity [18], catalysis [19], and photonic [20] characteristics may vary with the local elastic strain [9,21] and/or strain gradient (e.g. flexoelectric [22] effect). Such miniaturized experiments took off after the invention of the Atomic Force Microscope (AFM), and current examples include AFM/scanning tunneling microscopy (STM), nanoindentation, microfabrication based manipulators combined with *in situ* spectroscopies such as photoluminescence and Raman [21], cathodoluminescence [9], electron energy loss spectroscopy (EELS) [23] mappings, micro-electromechanical system (MEMS)/nano-electromechanical system (NEMS) lab-on-a-chip measurements, etc. Pillar 2 is key for verifying how the actual functional properties may change with elastic strain, as well as for the prototyping of practical ESE devices with overall current-voltage (I – V) responses in two- or three-terminal configurations. Generally speaking, future deep ESE devices are more likely to rely on MEMS-like geometrical designs and fab processes [20] where there are a lot more freely-suspended parts, actuated by piezo or electrostatic transducers, mimicking the “hundred tiny hands” of Feynman [24], rather than the more traditional thin-film deposition/etching/lift-off designs that produce more constrained geometries and rely on static epitaxial strain, which is limited to a few percent strains maximally (“shallow ESE”).

Pillar 3

Pillar 3 involves characterizing and modeling the mechanisms of inelastic stress relaxations [1,2,25] at realistic application temperatures over timescale of months to years [26,27]. For example, suppose one wants to keep Si strained at 5% elastic tension at 60 °C for 3 years, but finds that the imposed elastic strain is relaxed away after only 2 months, one would want to know whether this is likely caused by surface diffusional creep [28,29], dislocation nucleation [30,31], or crack propagation [32]. In such endeavor, one must rely on TEM [33–38] and synchrotron based experimental characterizations, as well as theory and modeling of the deformation mechanisms. While the length scale of *in situ* TEM observations matches that of molecular dynamics simulations, the accessible timescale of the latter is still off by many orders of magnitude. To address this challenge, accelerated timescale simulations technique and analytical framework have been developed

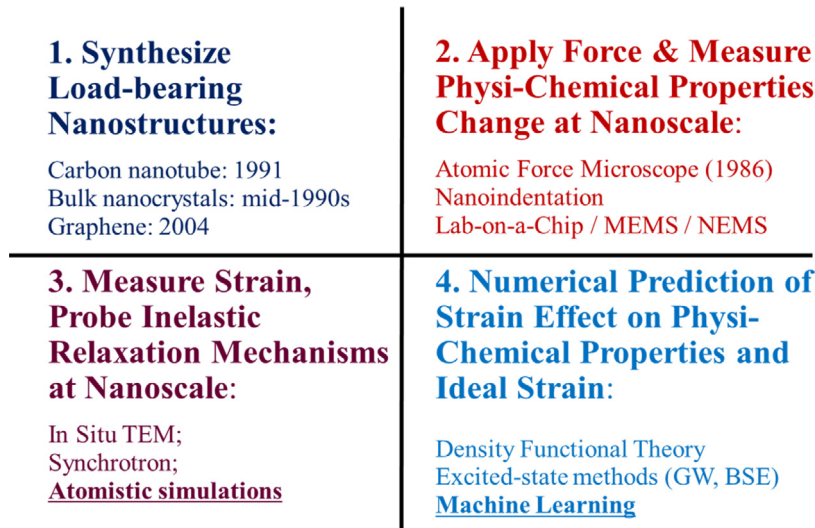


Fig. 1. Four pillars of Elastic Strain Engineering.

to study fundamental defect processes such as dislocation and crack nucleation [3] and coupled diffusive–displacive processes [26,27] by multi-scale simulations. Note that while Pillar 3 uses the same tools as traditional mechanics of materials research, the goal and philosophy are different in that one is not trying to utilize these deformation mechanisms for forming operations that motivated most traditional metallurgy studies, but to defeat these mechanisms in realistic conditions and “lock in” the high elastic strain energy, a metastable state of matter, for long-term utilization of functional properties. Pillar 3 is thus tasked with providing the stress (σ)-temperature (T)-service time(t)-scalescale(D) “safe operation envelope” for ESE devices.

Pillar 4

Pillar 4 is computational design based on first-principles calculations and ML constitutive relations [39,40]. One needs this pillar to obtain the 5-dimensional ideal strength surface embedded in 6D strain space, and to ask questions like: if we can shear in this crystallographic direction to maximally 70% of the ideal strength, how would the physical properties change and what would this allow one to do with respect to device figure-of-merit (FOM) [41]? The device FOM is usually a lumped parameter of thermal conductivity, carrier mobility, dielectric breakdown strength, etc. all of which depend on the strain tensor ϵ . Generally speaking, there is no symmetry principle that says any physical property A , including the FOM, is optimized at the stress-free condition $\epsilon = 0$: $\partial A / \partial \epsilon \neq 0$. Thus, just like chemical alloying, where the composition of the liquid melt \mathbf{X} is continuously tuned to achieve superior properties after solidification (bronze age \rightarrow iron age \rightarrow silicon age), one can always tune the elastic strain tensor to improve FOM. So in this sense, the 6D strain space is equivalent to a 7-element (septenary) alloy, and we can develop regime maps for A like the “isothermal phase diagrams” [42]. ESE with MEMS and technology computer-aided design (TCAD) has a further advantage compared to chemical doping in semiconductor devices, as the chemical doping profile has to be achieved by ion implantation or high-temperature diffusion that can only be done in the Fab. The ESE $\epsilon(\mathbf{x}, t)$ pattern generated by MEMS “hundred tiny hands” [24] may be adjusted dynamically during service, offering rich functional flexibilities. Continuum TCAD modeling is required to unravel these design choices based on first-principles machine-learned (FPML) constitutive relation [40,42], and geometric and

topological optimizations (TO) of the device geometry need to be carried out.

Some concrete examples of ESE mechanical design and materials discovery are given. One theoretical work proposes to harvest solar energy using strain-engineered atomic sheets with tunable bandgap as funnels of charge-neutral excitons [43]. The basic idea is that with the bandgap varying linearly with the local strain, the $1/r$ deformation potential on electron and hole carriers creates artificial 2D atoms like the hydrogen atom model. The $1/r$ strain field thus induces novel behavior in photon absorption and energy-charge transport. Like a funnel the nonlinear deformation potential drives the charge-neutral electron–hole pair toward the indentation center, making the charge-separation region potentially much more localized than the intrinsic photon-absorption region of the device material. This strain-induced energetic quasiparticle transport and exciton funneling effect has been later verified experimentally in 2D MoS₂ with photoluminescence mapping [21], and bent 3D ZnO microwires with cathodoluminescence measurement [9] (Pillar 1 and 2).

The second example deals with how elastic strain affects the topology of band structures. The field of electronic materials has seen a revolution with the introduction of the band topology in reciprocal space, with newly discovered classes of materials known as topological insulators, metals and superconductors. These materials have been shown to host electronic states robust against scattering by many types of disorder that strongly affect conventional metals and semiconductors. In 2014, we predicted that monolayer 1T'-WTe₂ under appropriate tensile strains is a 2D topological insulator with perfect edge quantum conductance [44], while bilayer WTe₂ is not. This was later verified by multiple experimental groups [45–47]. This joined the field of 2D materials and topological materials, often enabled by few-percent elastic strain [48]. Similar transitions have also been predicted for topological metals [49,50], and materials with so-called Mexican-Hat band structures which are predicted to give giant photonic responses in the infrared [51].

Since the strain ϵ is continuous 6D variable and the wavevector \mathbf{k} is 3D variable, a full description of how the electronic or phonon band structure of a material $e_n(\mathbf{k}; \epsilon)$ depends on strain, where n is the band index, is a non-trivial computational task. A simple tabulation approach would hardly work in even storing the data (20 grid points in each axis would require 20⁹ or 4 terabytes per band), and computing these data from first-principles, like the many-body GW approach, can be quite expensive. It turns

out that with a good ML model armed with active learning [52] and transfer learning capabilities, only 10^4 DFT calculations with 10^3 GW calculations are necessary to represent $e_n(\mathbf{k}; \boldsymbol{\epsilon})$ well, which are well within the reach of research groups. We have recently developed a method that invokes NNs and utilizes a limited amount of *ab initio* data for the training of a NN model, predicting the bandgap within an accuracy of 8 meV [39]. On top of this, attempts have been made in developing a more versatile ML framework that adopts convolutional blocks, data fusion, and active learning to discover the indirect-to-direct bandgap transition and Mott transition in a material by scanning the entire strain space. Through this framework, we recently achieved enhanced performance in every front [39], including more accurate bandgap and band structure prediction, band extrema detection, and effective mass prediction that requires computing the second derivative of $\partial^2 e_n(\mathbf{k}; \boldsymbol{\epsilon}) / \partial \mathbf{k} \partial \mathbf{k}$ [40]. From previous experience with developing NN interatomic potentials [53,54], we know that deep NN can have a numerical noise problem: sometimes even when the predicted energy gives low mean absolute error (MAE), the predicted forces which are the first derivatives can have significant MAE. Here, the fact that even the second derivative $\partial^2 e_n(\mathbf{k}; \boldsymbol{\epsilon}) / \partial \mathbf{k} \partial \mathbf{k}$ can be predicted accurately bodes well for the FPML constitutive relation approach using NN representation [40,42].

We have applied NN based model to represent band structure of lattices in ultra-large strain space, and classify band structure topology transitions [39]. Elastic strain provides a huge *material genomic* space to tune their properties and push the limit of device performance, by TCAD based on FPML constitutive relation [40,42], to provide the requisite bandgap and band alignment patterns, dopant charging levels, carrier effective mass, etc. data objects for carrying out finite-element simulations and predicting the *I-V* of deeply strained device. These simulations are crucial for understanding the fundamental limiting factors (such as thermal conduction limit), thus driving evolutionary or revolutionary design. In this endeavor ML allows easy visualization of the key physical metrics [39] and performing Pareto-front multi-objective optimization [40]. ML enables the construction of phase diagram like visualizations of the different regimes of indirect bandgap and direct bandgap semiconductors and direct/indirect metals, and mathematically trace the transition-strain ridge lines and cusps, with automatically labeled symmetry notations [39,42]. Some materials in the topologically trivial phase may transform to a topologically non-trivial phase under external strain, as predicted in 2014 for topological insulators [44,48] and 2016 for topological metals [49,50], so that the exotic topological properties could be harnessed dynamically by mechanical design.

One can expand the concept of “strain engineering” beyond elastic strains to include inelastic strain engineering, such as ferroelastic [55,56] and ferroelectric [57,58] phase transitions in 2D [59] and 3D materials. The difference between elastic and inelastic strains is that the former still resides in a single convex energy basin despite the large strain magnitude, while the latter traverses at least two convex energy basins, with energy-concave “saddle” region in between. In energy technology applications (superconducting cables, catalysts, batteries etc.) that requires kilogram-scale, if not ton or kiloton scale materials, a nanocomposite approach is often necessary to scale up ESE to kilogram-level bulk materials. For example, individual free-standing nanowires are known to have ultrahigh elastic strain limits, but exploiting their intrinsic mechanical properties in bulk composites has proven to be difficult and is thus often called the “valley of death”. In order to reach deep elastic strains for at least one phase component of kilogram-scale nanocomposite, we have established a material design principle of “strain matching”, using the martensitic transformation strain of one phase to match the true elastic strain of the other phase. We proposed

that in order to achieve large elastic strains without inelastic relaxation in one phase (the nanowire fillers), it is necessary to match its elastic strain range with the pseudoelastic (martensitic phase transformation) strain range of the matrix phase, that is usually much gentler on their interfaces than dislocation slip at the atomic scale, to preserve the intrinsically large elasticity limit of the nano-fillers [10]. This is because at the atomic scale (i.e. in between two adjacent atomic planes), while the phase transformation strain is truly on the order of 10%, the inelastic strain from dislocation slip b/d_0 is often greater than 100%, so dislocation plasticity is a much sharper knife if piled up at the interface, and easily triggers inelastic relaxation inside the nano-fillers [10] that we aim to keep elastically strained. By engineering the microstructure and residual stress to couple the large true elasticity of Nb nanowires with the pseudoelasticity of a NiTi shape memory alloy, an *in situ* composite is developed that possesses a large quasi-linear elastic strain of over 6%, a low Young’s modulus of ~ 28 GPa, and a high yield strength of ~ 1.65 GPa [10]. As verified by *in situ* synchrotron diffractions, kilogram-scale nanowires were stretched to 6% elastic strain reversibly. This residual elastic strain has been shown to lead to superior Niobium-based superconductors with enhanced T_C and critical magnetic fields [18]. In 2021, we further demonstrated deep ESE of kilogram-scale Ti-Ni-Fe metallic glass with the same strain-matching principle [60], approaching the ideal strength of metallic glasses [12,29]. As metallic glasses have been developed historically for magnetic response used in e.g. transformer cores, how the magnetic properties of metallic glasses can be strain-engineered deserves further study. In the future, the inelastic/elastic strain-matching design should open up new avenues for developing functional nano-composites by coupling strain-matching “loader” with 1-D, 0-D and 2-D nano-components for ESE at the kilogram to kiloton scales, which is required for most energy technology (ET) applications.

For information technology (IT) applications such as electronics, photonics and quantum sensors and networks, to demonstrate the scalability of ESE, in 2021 we have dynamically strained *arrays* of few μm -length single crystal diamond bridges to 6% tensile elastic strain reversibly (Fig. 2C–E) [61]. In the future, each micro-bridge may contain thousands of nanoscale transistors or quantum sensors. Wafer-scale integration with piezoelectric, electrostatic or thermal-expansion based micro-actuators from MEMS technology is clearly feasible with this demonstration. In the future these transistors and quantum sensors can then operate in the deep ESE regime, defined by $>5\%$ tensile or shear strains, over period of months or years. Diamond is the “Mount Everest” of electronic materials, with extreme carrier mobility, thermal conductivity and dielectric breakdown strength. The fact that microfabricated diamond can sustain $>6\%$ tensile elastic strain bodes well for the deep ESE of *all* ultra-wide bandgap semiconductors [41]. Before this work, in 2016 Yang Lu and team have already demonstrated Si single crystal wires can sustain $>13\%$ tensile elastic strain reversibly [8]. Unlike chemical doping or epitaxial strain, the team showed perfectly reversible unloading/reloading of such silicon microbridges dynamically, thus modifying physical properties on the fly and offering great functional flexibility for devices.

With Pillar 1 and 2 for diamond and silicon somewhat covered, and plenty of historical experience with Pillar 3 [32,62], we can move onto outlook of Pillar 4, the FPML-driven TCAD design of semiconductor devices. While deep ESE explores the full space of admissible (i.e. $\nabla \cdot \boldsymbol{\sigma} = 0$) nonlinear elastic strain patterns $\boldsymbol{\epsilon}(\mathbf{x}, t)$ that affects physical properties and device response, the complexity of controllably engineering materials properties by strains necessitates first-principles computations to firstly screen for a desirable FOM and then design an optimal straining pathway.

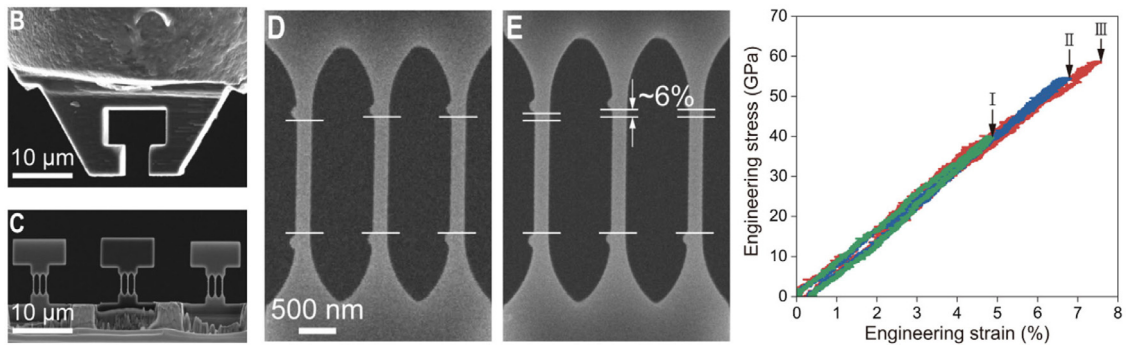


Fig. 2. Achieving large uniform tensile elasticity in arrays of microfabricated single-crystalline diamond. Source: Figures are taken from [61].

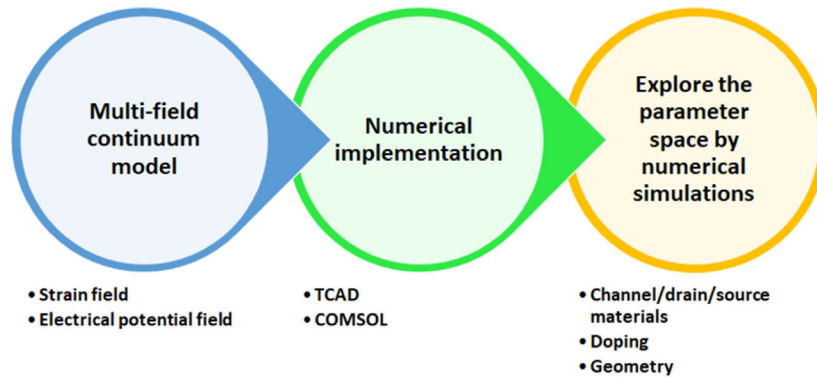


Fig. 3. General procedures for conducting multi-field continuum modeling for device performance evaluation and device design.

To map the 6D strain space fully, we will first combine ML and DFT calculations to guide strain engineering whereby electronic properties could be designed.

In ongoing works, we are combining this method with experimentally validated finite element (FEM) simulations to predict strain pathways that would reversibly transform an ultrawide-bandgap material such as diamond to a metalized state without phase transformation, paving the way for more extensive device-level simulations, depicted in Fig. 3. Phonon stability which defines the ideal strength surface in 6D strain space is a key boundary for such simulations, akin to the “Tresca yield surface”. Also, the nonlinear elastic stress–strain relation is provided by our FPML, which is used as input for the FEM simulation of admissible strain patterns $\nabla \cdot \sigma = 0$. For MOSFET, people define device FOMs such as the subthreshold swing, largest current driven by the transistor, dynamic power factor, and intrinsic delay time [63]. These as well as many other properties are suggested in the International Technology Roadmap for Semiconductors [64]. It is a natural development to incorporate the heterogeneous strain model into TCAD simulations, that solves the Poisson–Boltzmann equation, heat conduction equation and stress equilibrium equation simultaneously, out of which we will get the I – V and temperature distribution characteristics that can be directly compared with prototype experiments. Such integration advances the academic field of device simulations where models currently exist only for moderately strained channel materials [65]. The complexity of deep elastic strain effects, ranging from the impact of strain on process simulation to 3D effects and drain current enhancement in the quasi-ballistic transport regime of nanoscale transistors, makes TCAD simulation a challenging task. It is noted that in real semiconductor devices, there are other issues to be dealt with, including the contact resistance and imperfections aforementioned, and thus experimental verification is sorely needed.

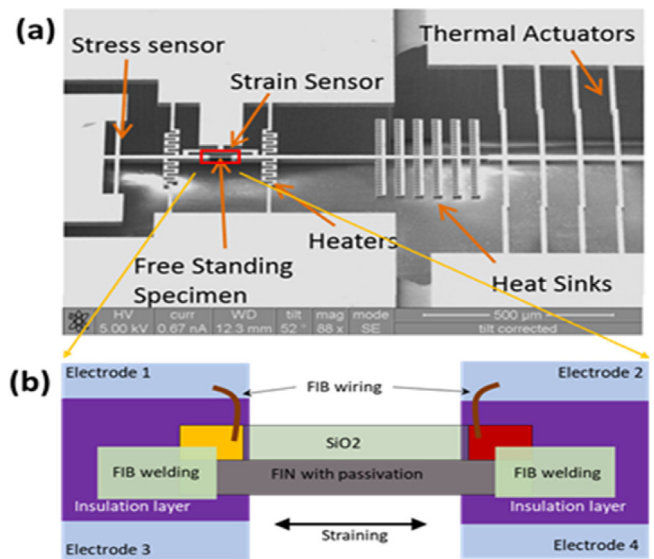


Fig. 4. Home-made in-situ TEM setup for simultaneous electrical measurement and straining for fin diode device. (a) MEMS chip for straining and electrical measurement; (b) Schematic of the proposed fin diode device after integration with the straining MEMS chip.

On the experimentation side, we are now working on coupling MEMS “tiny hands” [24] with fin-field-effect transistor (FinFET) like geometries [66–68]. The MEMS chip shown in Fig. 4a is designed and fabricated in-house, and the fin diodes are cut out and transferred to a MEMS chip as shown in Fig. 4a. The chip integrates actuators, heaters, stress/strain sensors and electrodes.

It is also compatible with in situ TEM and EELS characterizations for Pillar 3 and 2 diagnostics. Direct I - V measurements have been recently carried out while straining. Based on the experience built up with the fin diodes, we will move to more complex FinFET-like multi-terminal structures.

Historically, the field of ESE was populated by separate research communities focusing either on specific materials, or techniques. The first comprehensive symposium on ESE that cross-links different materials communities [69]: strained silicon, strained catalysts, strained multiferroics, strained atomic sheets, microscopy and nanomechanics, etc., were held at the MRS fall meeting in 2013. This well-attended symposium brought together different communities that use elastic strain to control material properties. The second MRS symposium on ESE was held in 2016 in Phoenix Arizona, organized by Bilge Yildiz. This forum of interdisciplinary discourse is essential for true advances in deep ESE. Mechanics of materials, both experimental mechanics and computational mechanics, will play a crucial role in this interdisciplinary endeavor, as should be clear from the text above.

In summary, 6-dimensional elastic strain is equivalent to, or even arguably superior to, the chemical degrees of freedom in a seven-element alloy, and can be used in conjunction with chemical composition design for reaching unprecedented material properties and device performance. A 5% tensile strained Si is not our “typical” Si, nor is 5% shear-strained Si. Thus, a new evolution of bronze \rightarrow iron \rightarrow silicon to ESE age is upon us, via *mechanical design*. By probing the fundamental mechanisms that materials can sustain shear or tensile strains exceeding 2%, 5%, or 10% without relaxation over extended time periods, one is pushing the frontiers of human control on materials. “Extreme mechanics” will be of vital importance in facilitating the successful implementation of ESE. We also showed that understanding how to vary the 6-dimensional elastic strain tensor opens up a vast area of functional materials design through the tuning of their physicochemical properties — electronic, optical, magnetic, photonic, etc. We demonstrated how to maintain large shear and tensile elastic strains over long timescales, by defeating the various mechanisms of inelastic relaxation, such as dislocation/twinning plasticity, fracture, and diffusional creep. Through the control of deep elastic strain field statically or dynamically, one can access a much larger parameter space for optimizing the functional properties of materials, giving a new meaning to Feynman’s 1959 statement “*there’s plenty of room at the bottom*”, where the room here stands for the ESE parametric freedom allowed by the “smaller is stronger” trend. Shallow strain engineering of a few percent by epitaxial deposition has already given us better lasers and faster computers, and is currently generating tens of billions of dollars benefits. This is really only the beginning, within the first two decades of the convergence of the four pillars, outlined in this article, necessary for rational ESE. In the long term, deep strain engineering with TCAD tools and first-principles machine-learned (FPML) constitutive relation, in close symbiosis with novel material discovery and MEMS-like device fabrication and characterizations, will lead to better information technologies and energy technologies, as the scalability of ESE for both wafer-scale IT and kilogram-scale ET materials have already been demonstrated experimentally.

EML webinar speakers, videos, and overviews can be found at <https://imechanica.org/node/24098>.

Declaration of competing interest

The authors declare that they have no known competing financial interests or personal relationships that could have appeared to influence the work reported in this paper.

References

- [1] T. Zhu, J. Li, Ultra-strength materials, *Prog. Mater. Sci.* 55 (2010) 710–757, <http://dx.doi.org/10.1016/j.pmatsci.2010.04.001>.
- [2] Q. Yu, Z.-W. Shan, J. Li, X. Huang, L. Xiao, J. Sun, E. Ma, Strong crystal size effect on deformation twinning, *Nature* 463 (2010) 335–338, <http://dx.doi.org/10.1038/nature08692>.
- [3] J. Li, The mechanics and physics of defect nucleation, *MRS Bull.* 32 (2007) 151–159, <http://dx.doi.org/10.1557/mrs2007.48>.
- [4] L. Huang, Q.-J. Li, Z.-W. Shan, J. Li, J. Sun, E. Ma, A new regime for mechanical annealing and strong sample-size strengthening in body centred cubic molybdenum, *Nature Commun.* 2 (2011) 547, <http://dx.doi.org/10.1038/ncomms1557>.
- [5] L. Tian, J. Li, J. Sun, E. Ma, Z.-W. Shan, Visualizing size-dependent deformation mechanism transition in Sn, *Sci. Rep.* 3 (2013) 2113, <http://dx.doi.org/10.1038/srep02113>.
- [6] T. Zhu, J. Li, S. Ogata, S. Yip, Mechanics of ultra-strength materials, *MRS Bull.* 34 (2009) 167–172, <http://dx.doi.org/10.1557/mrs2009.47>.
- [7] S.W. Bedell, A. Khakifirooz, D.K. Sadana, Strain scaling for CMOS, *MRS Bull.* 39 (2014) 131–137, <http://dx.doi.org/10.1557/mrs.2014.5>.
- [8] H. Zhang, J. Tersoff, S. Xu, H. Chen, Q. Zhang, K. Zhang, Y. Yang, C.-S. Lee, K.-N. Tu, J. Li, Y. Lu, Approaching the ideal elastic strain limit in silicon nanowires, *Sci. Adv.* 2 (2016) e1501382, <http://dx.doi.org/10.1126/sciadv.1501382>.
- [9] X. Fu, C. Su, Q. Fu, X. Zhu, R. Zhu, C. Liu, Z. Liao, J. Xu, W. Guo, J. Feng, J. Li, D. Yu, Tailoring exciton dynamics by elastic strain-gradient in semiconductors, *Adv. Mater.* 26 (2014) 2572–2579, <http://dx.doi.org/10.1002/adma.201305058>.
- [10] S. Hao, L. Cui, D. Jiang, X. Han, Y. Ren, J. Jiang, Y. Liu, Z. Liu, S. Mao, Y. Wang, Y. Li, X. Ren, X. Ding, S. Wang, C. Yu, X. Shi, M. Du, F. Yang, Y. Zheng, Z. Zhang, X. Li, D.E. Brown, J. Li, A transforming metal nanocomposite with large elastic strain, low modulus, and high strength, *Science* 339 (2013) 1191–1194, <http://dx.doi.org/10.1126/science.1228602>.
- [11] J. Frenkel, Zur Theorie der Elastizitätsgrenze und der Festigkeit kristallinischer Körper, *Z. Phys.* 37 (1926) 572–609, <http://dx.doi.org/10.1007/BF01397292>.
- [12] P. Zhao, J. Li, Y. Wang, Extended defects, ideal strength and actual strengths of finite-sized metallic glasses, *Acta Mater.* 73 (2014) 149–166, <https://doi.org/10.1016/j.actamat.2014.03.068>.
- [13] F. Liu, P. Ming, J. Li, Ab initio calculation of ideal strength and phonon instability of graphene under tension, *Phys. Rev. B* 76 (2007) 064120, <http://dx.doi.org/10.1103/PhysRevB.76.064120>.
- [14] C. Lee, X. Wei, J.W. Kysar, J. Hone, Measurement of the elastic properties and intrinsic strength of monolayer graphene, *Science* 321 (2008) 385–388, <http://dx.doi.org/10.1126/science.1157996>.
- [15] N.N. Klimov, S. Jung, S. Zhu, T. Li, C.A. Wright, S.D. Solares, D.B. Newell, N.B. Zhitenev, J.A. Strosio, Electromechanical properties of graphene drumheads, *Science* 336 (2012) 1557, <http://dx.doi.org/10.1126/science.1220335>.
- [16] M. Dao, N. Chollacoop, K.J. Van Vliet, T.A. Venkatesh, S. Suresh, Computational modeling of the forward and reverse problems in instrumented sharp indentation, *Acta Mater.* 49 (2001) 3899–3918.
- [17] J. Li, K.J. Van Vliet, T. Zhu, S. Yip, S. Suresh, Atomic mechanisms governing elastic limit and incipient plasticity in crystals, *Nature* 418 (2002) 307–310, <http://dx.doi.org/10.1038/nature00865>.
- [18] S. Hao, L. Cui, H. Wang, D. Jiang, Y. Liu, J. Yan, Y. Ren, X. Han, D.E. Brown, J. Li, Retaining large and adjustable elastic strains of kilogram-scale Nb nanowires, *ACS Appl. Mater. Interfaces* 8 (2016) 2917–2922, <http://dx.doi.org/10.1021/acsami.5b10840>.
- [19] J. Wu, L. Qi, H. You, A. Gross, J. Li, H. Yang, Icosahedral platinum alloy nanocrystals with enhanced electrocatalytic activities, *J. Am. Chem. Soc.* 134 (2012) 11880–11883, <http://dx.doi.org/10.1021/ja303950v>.
- [20] W. Jiang, R.N. Patel, F.M. Mayor, T.P. McKenna, P. Arrangoiz-Arriola, C.J. Sarabalis, J.D. Witmer, R. Van Laer, A.H. Safavi-Naeini, Lithium niobate piezo-optomechanical crystals, *Optica* 6 (2019) 845–853, <http://dx.doi.org/10.1364/OPTICA.6.000845>.
- [21] H. Li, A.W. Contryman, X. Qian, S.M. Ardakani, Y. Gong, X. Wang, J.M. Weisse, C.H. Lee, J. Zhao, P.M. Ajayan, J. Li, H.C. Manoharan, X. Zheng, Optoelectronic crystal of artificial atoms in strain-textured molybdenum disulphide, *Nature Commun.* 6 (2015) 7381, <http://dx.doi.org/10.1038/ncomms8381>.
- [22] J. Feng, L. Qi, J.Y. Huang, J. Li, Geometric and electronic structure of graphene bilayer edges, *Phys. Rev. B* 80 (2009) 165407, <http://dx.doi.org/10.1103/PhysRevB.80.165407>.
- [23] C. Su, M. Tripathi, Q.-B. Yan, Z. Wang, Z. Zhang, C. Hofer, H. Wang, L. Basile, G. Su, M. Dong, J.C. Meyer, J. Kotakoski, J. Kong, J.-C. Idrobo, T. Susi, J. Li, Engineering single-atom dynamics with electron irradiation, *Sci. Adv.* 5 (2019) eaav2252, <http://dx.doi.org/10.1126/sciadv.aav2252>.
- [24] R.P. Feynman, There’s plenty of room at the bottom, *Eng. Sci.* 23 (1960) 22–36.

- [25] J. Sun, L. He, Y.-C. Lo, T. Xu, H. Bi, L. Sun, Z. Zhang, S.X. Mao, J. Li, Liquid-like pseudoelasticity of sub-10-nm crystalline silver particles, *Nature Mater.* 13 (2014) 1007–1012, <http://dx.doi.org/10.1038/nmat4105>.
- [26] J. Li, S. Sarkar, W.T. Cox, T.J. Lenosky, E. Bitzek, Y. Wang, Diffusive molecular dynamics and its application to nanoindentation and sintering, *Phys. Rev. B* 84 (2011) 054103, <http://dx.doi.org/10.1103/PhysRevB.84.054103>.
- [27] W. Guo, Z. Wang, J. Li, Diffusive versus displacive contact plasticity of nanoscale asperities: Temperature- and velocity-dependent strongest size, *Nano Lett.* 15 (2015) 6582–6585, <http://dx.doi.org/10.1021/acs.nanolett.5b02306>.
- [28] Y. Chen, Z. Wang, X. Li, X. Yao, C. Wang, Y. Li, W. Xue, D. Yu, S.Y. Kim, F. Yang, A. Kushima, G. Zhang, H. Huang, N. Wu, Y.-W. Mai, J.B. Goodenough, J. Li, Li metal deposition and stripping in a solid-state battery via coble creep, *Nature* 578 (2020) 251–255, <http://dx.doi.org/10.1038/s41586-020-1972-y>.
- [29] L. Tian, Y.-Q. Cheng, Z.-W. Shan, J. Li, C.-C. Wang, X.-D. Han, J. Sun, E. Ma, Approaching the ideal elastic limit of metallic glasses, *Nature Commun.* 3 (2012) 609, <http://dx.doi.org/10.1038/ncomms1619>.
- [30] Q.-J. Li, B. Xu, S. Hara, J. Li, E. Ma, Sample-size-dependent surface dislocation nucleation in nanoscale crystals, *Acta Mater.* 145 (2018) 19–29, <https://doi.org/10.1016/j.actamat.2017.11.048>.
- [31] J. Li, Diffusive origins, *Nature Mater.* 14 (2015) 656–657, <http://dx.doi.org/10.1038/nmat4326>.
- [32] T. Zhu, J. Li, S. Yip, Atomistic configurations and energetics of crack extension in silicon, *Phys. Rev. Lett.* 93 (2004) 205504, <http://dx.doi.org/10.1103/PhysRevLett.93.205504>.
- [33] D.-G. Xie, Z.-J. Wang, J. Sun, J. Li, E. Ma, Z.-W. Shan, In situ study of the initiation of hydrogen bubbles at the aluminium metal/oxide interface, *Nature Mater.* 14 (2015) 899–903, <http://dx.doi.org/10.1038/nmat4336>.
- [34] A. Kushima, J.Y. Huang, J. Li, Quantitative fracture strength and plasticity measurements of lithiated silicon nanowires by in situ TEM tensile experiments, *ACS Nano* 6 (2012) 9425–9432, <http://dx.doi.org/10.1021/nn3037623>.
- [35] Y. Yang, A. Kushima, W. Han, H. Xin, J. Li, Liquid-like, self-healing aluminum oxide during deformation at room temperature, *Nano Lett.* 18 (2018) 2492–2497, <http://dx.doi.org/10.1021/acs.nanolett.8b00068>.
- [36] J.Y. Huang, L. Zhong, C.M. Wang, J.P. Sullivan, W. Xu, L.Q. Zhang, S.X. Mao, N.S. Hudak, X.H. Liu, A. Subramanian, H. Fan, L. Qi, A. Kushima, J. Li, In situ observation of the electrochemical lithiation of a single SnO₂ nanowire electrode, *Science* 330 (2010) 1515–1520, <http://dx.doi.org/10.1126/science.1195628>.
- [37] A. Kushima, K.P. So, C. Su, P. Bai, N. Kuriyama, T. Maebashi, Y. Fujiwara, M.Z. Bazant, J. Li, Liquid cell transmission electron microscopy observation of lithium metal growth and dissolution: Root growth, dead lithium and lithium flotsams, *Nano Energy* 32 (2017) 271–279, <http://dx.doi.org/10.1016/j.nanoen.2016.12.001>.
- [38] A. Kushima, T. Koido, Y. Fujiwara, N. Kuriyama, N. Kusumi, J. Li, Charging/discharging nanomorphology asymmetry and rate-dependent capacity degradation in li–oxygen battery, *Nano Lett.* 15 (2015) 8260–8265, <http://dx.doi.org/10.1021/acs.nanolett.5b03812>.
- [39] Z. Shi, E. Tsybalov, M. Dao, S. Suresh, A. Shapeev, J. Li, Deep elastic strain engineering of bandgap through machine learning, *Proc. Natl. Acad. Sci.* 116 (2019) 4117–4122, <http://dx.doi.org/10.1073/pnas.1818555116>.
- [40] E. Tsybalov, Z. Shi, M. Dao, S. Suresh, J. Li, A. Shapeev, Machine learning for deep elastic strain engineering of semiconductor electronic band structure and effective mass, *NPJ Comput. Mater.* 7 (2021) 1–10, <http://dx.doi.org/10.1038/s41524-021-00538-0>.
- [41] J.Y. Tsao, S. Chowdhury, M.A. Hollis, D. Jena, N.M. Johnson, K.A. Jones, R.J. Kaplar, S. Rajan, C.G. Van de Walle, E. Bellotti, C.L. Chua, R. Collazo, M.E. Coltrin, J.A. Cooper, K.R. Evans, S. Graham, T.A. Grotjohn, E.R. Heller, M. Higashiwaki, M.S. Islam, P.W. Juodawlkis, M.A. Khan, A.D. Koehler, J.H. Leach, U.K. Mishra, R.J. Nemanich, R.C.N. Pilawa-Podgurski, J.B. Shealy, Z. Sitar, M.J. Tadjer, A.F. Witulski, M. Wraback, J.A. Simmons, Ultrawide-bandgap semiconductors: Research opportunities and challenges, *Adv. Electron. Mater.* 4 (2018) 1600501, <https://doi.org/10.1002/aelm.201600501>.
- [42] Z. Shi, M. Dao, E. Tsybalov, A. Shapeev, J. Li, S. Suresh, Metallization of diamond, *Proc. Natl. Acad. Sci.* 117 (2020) 24634, <http://dx.doi.org/10.1073/pnas.2013565117>.
- [43] J. Feng, X. Qian, C.-W. Huang, J. Li, Strain-engineered artificial atom as a broad-spectrum solar energy funnel, *Nat. Photonics* 6 (2012) 866–872, <http://dx.doi.org/10.1038/nphoton.2012.285>.
- [44] X. Qian, J. Liu, L. Fu, J. Li, Quantum spin hall effect in two-dimensional transition metal dichalcogenides, *Science* 346 (2014) 1344–1347, <http://dx.doi.org/10.1126/science.1256815>.
- [45] Z. Fei, T. Palomaki, S. Wu, W. Zhao, X. Cai, B. Sun, P. Nguyen, J. Finney, X. Xu, D.H. Cobden, Edge conduction in monolayer WTe₂, *Nat. Phys.* 13 (2017) 677–682, <http://dx.doi.org/10.1038/nphys4091>.
- [46] S. Tang, C. Zhang, D. Wong, Z. Pedramrazi, H.-Z. Tsai, C. Jia, B. Moritz, M. Claassen, H. Ryu, S. Kahn, J. Jiang, H. Yan, M. Hashimoto, D. Lu, R.G. Moore, C.-C. Hwang, C. Hwang, Z. Hussain, Y. Chen, M.M. Ugeda, Z. Liu, X. Xie, T.P. Devereaux, M.F. Crommie, S.-K. Mo, Z.-X. Shen, Quantum spin Hall state in monolayer 1T'-WTe₂, *Nat. Phys.* 13 (2017) 683–687, <http://dx.doi.org/10.1038/nphys4174>.
- [47] S. Wu, V. Fatemi, Q.D. Gibson, K. Watanabe, T. Taniguchi, R.J. Cava, P. Jarillo-Herrero, Observation of the quantum spin hall effect up to 100 kelvin in a monolayer crystal, *Science* 359 (2018) 76–79, <http://dx.doi.org/10.1126/science.aan6003>.
- [48] X. Qian, L. Fu, J. Li, Topological crystalline insulator nanomembrane with strain-tunable band gap, *Nano Res.* 8 (2015) 967–979, <http://dx.doi.org/10.1007/s12274-014-0578-9>.
- [49] Z. Zhu, M. Li, J. Li, Topological semimetal to insulator quantum phase transition in the Zintl compounds Ba₃X (X = Si, Ge), *Phys. Rev. B* 94 (2016) 155121, <http://dx.doi.org/10.1103/PhysRevB.94.155121>.
- [50] Z. Zhu, G.W. Winkler, Q. Wu, J. Li, A.A. Soluyanov, Triple point topological metals, *Phys. Rev. X* 6 (2016) 031003, <http://dx.doi.org/10.1103/PhysRevX.6.031003>.
- [51] H. Xu, J. Zhou, H. Wang, J. Li, Giant photonic response of mexican-hat topological semiconductors for mid-infrared to terahertz applications, *J. Phys. Chem. Lett.* 11 (2020) 6119–6126, <http://dx.doi.org/10.1021/acs.jpcclett.0c01552>.
- [52] D. Morgan, G. Pilania, A. Couet, B.P. Uberuaga, C. Sun, J. Li, Machine learning in nuclear materials research, *Curr. Opin. Solid State Mater. Sci.* (2021) in press.
- [53] S.T. Lam, Q.-J. Li, R. Ballinger, C. Forsberg, J. Li, Modeling LiF and FLiBe molten salts with robust neural network interatomic potential, *ACS Appl. Mater. Interfaces* 13 (2021) 24582–24592, <http://dx.doi.org/10.1021/acssami.1c00604>.
- [54] Q.-J. Li, E. Küçükbenli, S. Lam, B. Khaykovich, E. Kaxiras, J. Li, Development of robust neural-network interatomic potential for molten salt, *Cell Rep. Phys. Sci.* 2 (2021) 100359, <https://doi.org/10.1016/j.xcrp.2021.100359>.
- [55] W. Li, J. Li, Ferroelasticity and domain physics in two-dimensional transition metal dichalcogenide monolayers, *Nature Commun.* 7 (2016) 10843, <http://dx.doi.org/10.1038/ncomms10843>.
- [56] J. Zhou, H. Xu, Y. Li, R. Jaramillo, J. Li, Opto-mechanics driven fast martensitic transition in two-dimensional materials, *Nano Lett.* 18 (2018) 7794–7800, <http://dx.doi.org/10.1021/acs.nanolett.8b03559>.
- [57] Q. Yang, M. Wu, J. Li, Origin of two-dimensional vertical ferroelectricity in WTe₂ bilayer and multilayer, *J. Phys. Chem. Lett.* 9 (2018) 7160–7164, <http://dx.doi.org/10.1021/acs.jpcclett.8b03654>.
- [58] J. Zhang, Y. Mao, D. Wang, J. Li, Y. Wang, Accelerating ferroic ageing dynamics upon cooling, *NPG Asia Mater.* 8 (2016) e319, <http://dx.doi.org/10.1038/am.2016.152>.
- [59] W. Li, X. Qian, J. Li, Phase transitions in 2D materials, *Nat. Rev. Mater.* (2021) 1–18, <http://dx.doi.org/10.1038/s41578-021-00304-0>.
- [60] J. Zhang, Y. Liu, H. Yang, Y. Ren, L. Cui, D. Jiang, Z. Wu, Z. Ma, F. Guo, S. Bakhtiar, F. Motazedian, J. Li, Achieving 5.9% elastic strain in kilograms of metallic glasses: Nanoscopic strain engineering goes macro, *Mater. Today* 37 (2020) 18–26, <http://dx.doi.org/10.1016/j.mattod.2020.02.020>.
- [61] C. Dang, J.-P. Chou, B. Dai, C.-T. Chou, Y. Yang, R. Fan, W. Lin, F. Meng, A. Hu, J. Zhu, J. Han, A.M. Minor, J. Li, Y. Lu, Achieving large uniform tensile elasticity in microfabricated diamond, *Science* 371 (2021) 76–78, <http://dx.doi.org/10.1126/science.abc4174>.
- [62] W. Cai, V.V. Bulatov, J. Chang, J. Li, S. Yip, Chapter 64 dislocation core effects on mobility, *Dislocations Solids* 12 (2005) [http://dx.doi.org/10.1016/S1572-4859\(05\)80003-8](http://dx.doi.org/10.1016/S1572-4859(05)80003-8).
- [63] G. Pizzi, M. Gibertini, E. Dib, N. Marzari, G. Iannaccone, G. Fiori, Performance of arsenene and antimonene double-gate MOSFETs from first principles, *Nature Commun.* 7 (2016) 12585, <http://dx.doi.org/10.1038/ncomms12585>.
- [64] P. Gargini, GaAs IC Symposium. IEEE Gallium Arsenide Integrated Circuits Symposium. 22nd Annual Technical Digest 2000. (Cat. No.00CH37084). 3–5.
- [65] L. Smith, TCAD Modeling of Strain-Engineered MOSFETs. MRS Online Proceedings Library (OPL) 913, 2006, <http://dx.doi.org/10.1557/PROC-0913-D05-05>.
- [66] X. Zhao, J.A. del Alamo, A nanometer-scale vertical-sidewall reactive ion etching of ingaas for 3-d III-V MOSFETs, *IEEE Electron Device Lett.* 35 (2014) 521–523, <http://dx.doi.org/10.1109/LED.2014.2313332>.
- [67] A. Vardi, W. Lu, X. Zhao, J.A. del Alamo, A nanoscale mo ohmic contacts to III–V fins, *IEEE Electron Device Lett.* 36 (2015) 126–128, <http://dx.doi.org/10.1109/LED.2014.2386311>.
- [68] X. Zhao, A. Vardi, J.A. del Alamo, Fin-width scaling of highly doped InGaAs fins, *IEEE Trans. Electron Devices* 66 (2019) 2563–2568, <http://dx.doi.org/10.1109/TED.2019.2912618>.
- [69] J. Li, Z. Shan, E. Ma, Elastic strain engineering for unprecedented materials properties, *MRS Bull.* 39 (2014) 108–114, <http://dx.doi.org/10.1557/mrs.2014.3>.